Slow and Incomplete Inactivations of Voltage-gated Channels Dominate Encoding in Synthetic Neurons

Hsiaolan Hsu, Emily Huang, Xian-cheng Yang,* Andreas Karschin,‡ Cesar Labarca, Antonio Figl,§ Begonia Ho,¶ Norman Davidson, and Henry A. Lester

Division of Biology 156-29 and §Division of Chemistry and Chemical Engineering, California Institute of Technology, Pasadena, California 91125 USA

ABSTRACT Electrically excitable channels were expressed in Chinese hamster ovary cells using a vaccinia virus vector system. In cells expressing rat brain IIA Na^+ channels only, brief pulses (< 1 ms) of depolarizing current resulted in action potentials with a prolonged (0.5–3 s) depolarizing plateau; this plateau was caused by slow and incomplete Na^+ channel inactivation. In cells expressing both Na^+ and *Drosophila* Shaker H4 transient K^+ channels, there were neuron-like action potentials. In cells with appropriate Na^+/K^+ current ratios, maintaining stimulation produced repetitive firing over a 10-fold range of frequencies but eventually led to "lockup" of the potential at a positive value after several seconds of stimulation. The latter effect was due primarily to slow inactivation of the K^+ currents. Numerical simulations of modified Hodgkin-Huxley equations describing these currents, using parameters from voltage-clamp kinetics studied in the same cells, accounted for most features of the voltage trajectories. The present study shows that insights into the mechanisms for generating action potentials and trains of action potentials in real excitable cells can be obtained from the analysis of synthetic excitable cells that express a controlled repertoire of ion channels.

INTRODUCTION

The electrical and chemical excitability of neurons is controlled by a large repertoire of membrane proteins, including ion channels activated by changes in potential, channels activated by extracellular and intracellular ligands, seven-helix receptors coupled to G proteins, transporters, and ion pumps. These excitability proteins generally allow neurons to generate series of nerve impulses whose temporal pattern reflects various stimuli and modulatory influences. At present, several major approaches are available to analyze the contribution of a particular channel, receptor, or transporter to impulse firing patterns: 1) pharmacological activation and elimination, 2) antisense suppression of a particular protein, and 3) numerical modeling based on channel gating kinetics. We introduce an additional approach based on heterologous expression of foreign excitability proteins, in this case voltage-dependent channels. We contend that the new approach aids in hypothesis testing and enables the construction of entirely new classes of excitable cells.

A minimum requirement for the generation of a neuron-like action potential (Hodgkin and Huxley, 1952) would be the presence of one Na^+ channel type and one K^+ channel type (a possible exception is provided by some nodes of Ranvier, which lack K^+ channels) and a means to maintain an appropriate resting potential. Vaccinia virus expression systems are capable of expressing several channel types simultaneously at the required levels and were therefore employed (Leonard et al., 1989; Karschin et al., 1991a; Yang et al., 1992).

All-or-none action potentials were indeed recorded in these simple synthetic neurons. Interestingly, however, we have found that the encoding properties of these cells are more complex than would be expected simply on the basis of voltage-clamp data on the expressed Na^+ and K^+ currents on a millisecond time scale. Recent data emphasize that both endogenous and heterologously expressed mammalian Na^+ currents (Llinás, 1988; Krafte et al., 1988, 1990; Zhou et al., 1991) and expressed *Drosophila* Shaker H4 currents (Iverson and Rudy, 1990; Hoshi et al., 1991) display slow and incomplete inactivation on a time scale of seconds. In an iterative series of experiments involving electrophysiological measurements and numerical simulation, we found that these slow properties help to determine the voltage trajectories in the synthetic neurons. Slow inactivation of transient K^+ currents could play a role in the encoding properties of real neurons as well.

Received for publication 16 March 1993 and in final form 16 June 1993.

Address reprint requests to Dr. Henry A. Lester at the Division of Biology 156-29, California Institute of Technology, Pasadena CA 91125. BITNET Lester @ Caltech; Tel.: 818-356-4946; Fax: 818-564-8709.

*Present address: Medical Research Division, American Cyanamid Corp., Pearl River, NY 10965.

‡Present address: Abteilung Membranbiophysik, Max-Planck Institut für biophysikalische Chemie, D-34 Gottingen-Nikolausberg, Germany.

¶Present address: Department of Pharmacology, University of Texas Southwestern Medical Center, 5323 Harry Hines Blvd., Dallas TX 75235-9041.

0006-3495/93/09/1196/11 $2.00

MATERIALS AND METHODS

Viruses and plasmids

The vaccinia virus vTF7–3 encodes the bacteriophage T7 RNA polymerase under the control of a vaccinia virus promoter (Elroy-Stein et al., 1989). Na^+ and K^+ channel cDNAs were inserted into the plasmid pTM1 (Moss et al., 1990) downstream from the T7 promoter, T7 hairpin, and encephalomyocarditis virus 5′-untranslated region.

Construction and expression of the Na^+ channel plasmid, pTM1NaIIA, has been described by Yang et al. (1992). The cDNA encoded Leu at position

860. The Shaker H4 cDNA was furnished by M. Tanouye and mutated by Klaiber et al. (1990) to provide an *NcoI* site at the initial ATG codon. The *NcoI*/*EcoRI* fragment was excised from pBluescript (Stratagene Cloning Systems, La Jolla, CA), transferred to pTM1, and named pTM1KH4. A DNA-Lipofectin (GIBCO-BRL Life Technologies, Gaithersburg, MD) complex was formed by mixing plasmid DNA with Lipofectin and incubating for 20 min at room temperature.

Expression

CHO cells were plated on 35-mm dishes. 16–20 h later, cells were rinsed with phosphate-buffered saline containing 1 mM $MgCl_2$ and 0.1% bovine serum albumin and were infected with vTF7–3 at a multiplicity of infection (MOI) of 10 for 30–35 min. Cells were then exposed to serum-free culture medium plus 100 units/ml penicillin, 100 units/ml streptomycin, 2 mM glutamine, nonessential amino acids, and DNA-Lipofectin complex and were incubated for 24 h. Amounts of pTM1NaIIA plasmid DNA, pTM1KH4 plasmid DNA, and Lipofectin were 3.2, 0.4, and 9.6 μg, respectively. Cells were then maintained in culture medium plus 5% bovine serum albumin.

Electrophysiology

Culture dishes containing infected/Lipofected cells were rinsed twice with bath solution (145 mM NaCl, 5 mM KCl, 1.8 mM $CaCl_2$, 1.2 mM $MgCl_2$, 10 mM 4-(2-hydroxyethyl)-1-piperazineethanesulfonic acid (HEPES), pH 7.4). For solutions with reduced external NaCl, tetraethylammonium chloride was substituted. Patch pipettes were pulled from thick-walled glass tubing (Sutter Instrument Co., Novato, CA) on a Sutter P-80 puller and filled with intracellular solution (120 mM KCl, 25 mM KCl, 5 mM NaCl, 1 mM $MgCl_2$, 10 mM HEPES, 5 mM EGTA, pH 7.2). Tip resistances were 2–5 MΩ. Recordings were performed with an Axopatch-1D (Axon Instruments, Foster City, CA) circuit under the control of pCLAMP software (Axon Instruments) running on MS-DOS computers. Series resistance compensation was not employed. Tetrodotoxin (300 nM) was applied by pressure from the tip of a pipette positioned ~5 μm from the cell. Records shown are typical of at least five cells in each case.

Numerical simulations

Simulations were performed on UNIX workstations running the NEURON program (Hines, 1989) for a single-compartment cell. We employed the descriptions introduced by Hodgkin and Huxley (1952) with the following extensions. The Na^+ conductance is usually described as $\bar{g}m^3h$, where $\bar{g}$ is the maximal Na^+ conductance and m and h (the activation and inactivation parameters, respectively) vary between 0 and 1. For the present work, we modified the $\bar{g}m^3h$ formalism to include two inactivation parameters h_1 (fast) and h_2 (slow). The modified term is $\bar{g}m^3[\epsilon + h_1(1 - \epsilon)]h_2$. Other formalisms, for instance a simple addition of terms in $\bar{g}m^3h_1$ and $\bar{g}m^3h_2$, would also be acceptable for our Na^+ current data; the present formalism was chosen because it served well for simulations of both the Na^+ and K^+ conductances. In the following equations, I is membrane current, C_M is membrane capacitance, V is potential, and E_i is the Nernst potential for conductance i (Na^+, K^+, or leak):

$$I = C_M \frac{dV}{dt} + \sum I_i,$$

$$I_i = \bar{g}_i(V - E_i)m_i^3[\epsilon_i + h_{1i}(1 - \epsilon_i)]h_{2i},$$

$$\frac{dm_i}{dt} = \frac{m_{\infty i} - m_i}{\tau_{mi}},$$

$$\frac{dh_i}{dt} = \frac{h_{\infty i} - h_i}{\tau_i}.$$

For each τ, we define

$$\tau = 1/(\alpha + \beta).$$

For the leakage conductances, we define

$$m_{leak} = h_{leak} = 1; \qquad E_{leak} = -10 \text{ mV}.$$

The potentials are in millivolts and the times are in milliseconds. Cell areas were calculated from cell capacitance, using the value of 0.01 pF/(μm)^2. Cell area ranged from 10 to 20 μm^2 and averaged 12.3 μm^2.

RESULTS

We employed cDNA clones for the rat brain IIA Na^+ channel (Auld et al., 1988, 1990) and for the *Drosophila* Shaker H4 transient K^+ channel (Kamb et al., 1987; Iverson et al., 1988). To express the channels, cells were infected by a vaccinia virus expressing the bacteriophage T7 RNA polymerase and were also transfected by plasmids containing the channel cDNA downstream from the T7 promoter and the 5′-untranslated region of the encephalomyocarditis virus (Elroy-Stein et al., 1989). Control ("mock transfection") experiments utilized identical virus and plasmid vectors, but the cDNA encoded β-galactosidase rather than a channel.

In voltage-clamp experiments, mock-transfected control cells displayed little or no voltage-dependent currents (Fig. 1 *A*). Cells transfected with either the Na^+ or K^+ channel plasmids displayed only Na^+ or K^+ currents, respectively (Fig. 1, *B* and *C*), as expected from previous studies on expression using the highly efficient infection-transfection procedure (Yang et al., 1992) and related vaccinia expression systems (Leonard et al, 1989; Karschin et al., 1991a,1991b). Cells transfected with both the Na^+ and K^+ channel plasmids displayed both the inward and outward voltage-dependent currents appropriate to both channel types (Fig. 1 *D*). The peak current densities ranged from 100 to 450 pA/pF for Na^+ (at −10 mV) and from 100 to 700 pA/pF for K^+ (+50 mV). These values are likely to be underestimates, because we did not employ series resistance compensation.

The present analysis concerns data obtained when these cells were studied with current-clamp recording. This arrangement models the situation in a real neuron as it responds to synaptic stimuli from other cells.

Cells expressing Na^+ channels only

Fig. 2 *A* illustrates the voltage trajectory in a cell subjected to a brief (0.5 ms) pulse of outward (depolarizing) current, superimposed on a steady hyperpolarizing current to maintain the membrane potential at a level more negative than −70 mV in order to eliminate Na^+ current inactivation. In nearly all cells studied, the response began with a rapid depolarization to a potential more positive than +50 mV.

The subsequent voltage trajectory resembled cardiac rather than a neuronal action potential. A few milliseconds after reaching its peak, the membrane potential became less positive, then repolarized much more slowly for a variable period of several hundred milliseconds to several seconds (Fig. 2 *A*, *traces 1* through *5*). In experiments with timed

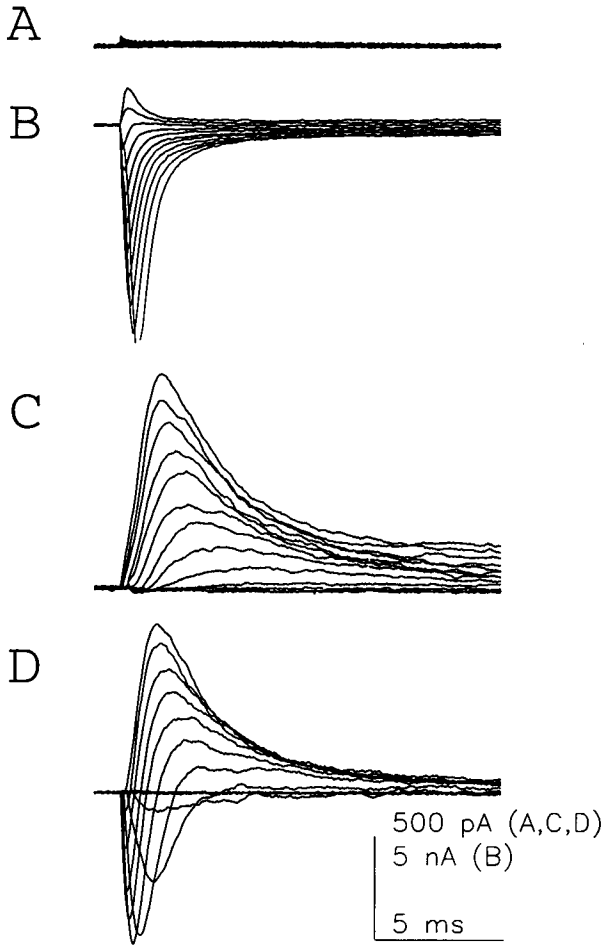

FIGURE 1 Voltage-clamp records on a millisecond time scale. Records from four different cells, illustrating the expression combinations used in these experiments. Each cell was infected with vTF7–3 and transfected with various plasmids based on pTM1. (*A*) Control cell. Transfection with pTM1lac, encoding β-galactosidase. There are no voltage-dependent currents. (*B*) Transfection with pTM1NaIIA, encoding the Na^+ channel. (*C*) Transfection with pTM1KH4, encoding the K^+ channel. (*D*) Transfection with both pTM1NaIIA and pTM1KH4. In all panels, leakage currents have been subtracted offline. In *A*, *C*, and *D* records were obtained with a holding potential of −70 mV and test potentials in 10-mV increments between −60 and +60 mV; vertical calibration, 500 pA. In *B* conditions were chosen to give large Na^+ channel currents and to reveal the small noninactivating component of Na^+ current, as follows. 1) Holding potential was −100 mV, to eliminate partial inactivation. 2) A cell with higher than average currents (>10 nA peak) was chosen. These large currents vitiated high-fidelity voltage-clamp feedback and saturated the recording equipment. 3) Passive and capacitive components were subtracted online in a P/4 procedure. 4) A further offline correction of 0.3 nS was required to produce zero current near the reversal potential, and this was subtracted from all the records. Test potentials in *B* are at 10-mV increments between −20 and +80 mV; vertical calibration is 5 nA.

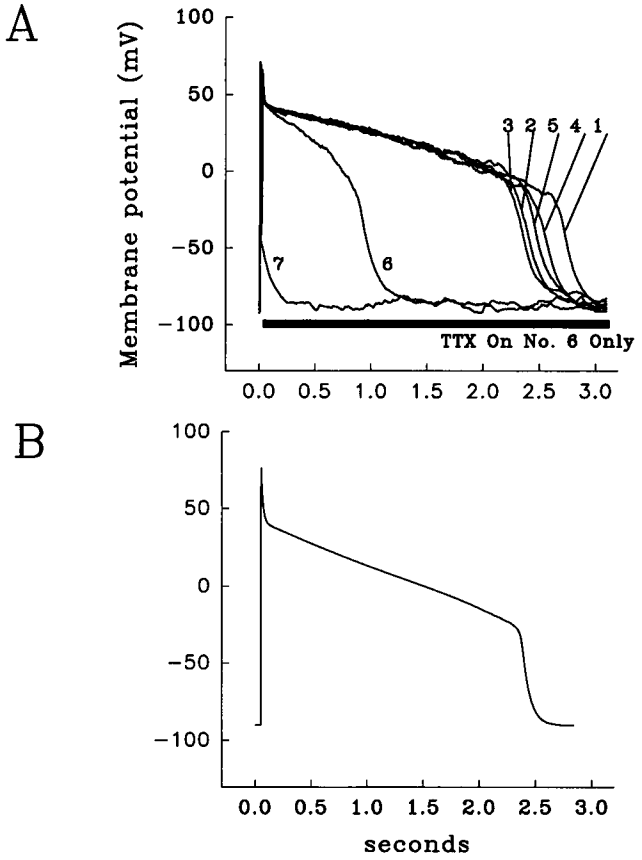

FIGURE 2 Analysis of the action potentials in a cell expressing only Na^+ channels and an unusually prolonged plateau. (*A*) Voltage recordings during a current-clamp experiment. The trial comprised seven episodes, at intervals of 10 s. In each case, the action potential was evoked by a depolarizing pulse at time zero (0.5 ms, 0.7 nA, superimposed on a −20-pA steady current). During episode 6, TTX (300 nM) was applied from a puffer pipette for the period indicated by the bar. TTX application began 24 ms after the depolarizing pulse; therefore the early peak currents were not affected, but the prolonged, small currents were blocked. The TTX pulse shortened the plateau, indicating that it is produced by the Na^+ channels. The Na^+ channels remained blocked during episode 7 but recovered over the next minute as the TTX diffused away (not shown). (*B*) Simulated plateau; $\bar{g}_{Na}$ = 47.5 pS/(μm)², $\bar{g}_K$ = 0, $\bar{g}_{leak}$ = 0.15 pS/(μm)².

puffs of tetrodotoxin, we showed that these plateaus depend directly on Na^+ channels rather than on any possible small endogenous voltage-dependent properties that might have been overlooked in previous studies (Fig. 2 *A*, *traces 6* and *7*). There was a noticeable effect of expression level on the duration of the plateau: for cells with average peak Na^+ currents of 2 nA, the plateau lasted <1 s; for currents near 10 nA, the plateau lasted >3 s. The variations among trials on the same cell (Fig. 2 *A*) were probably caused by both (*a*) fluctuations in the seal resistance and (*b*) spontaneous fluctuations in the relatively small numbers of Na^+ channels open during the plateau.

Action potential waveforms with prolonged plateaus are typical of cardiac cells, such as Purkinje fibers and ventricular myocytes, and are rarely observed in neurons. However, similar plateaus have been observed in previous experiments where (*a*) only Na^+ channels were stimulated, (*b*) voltage-dependent K^+ channels were eliminated, and (*c*) resting conductances were very low (Chandler and Meves, 1970d). The most likely reason for the plateau is that Na^+ channels do not inactivate completely. One source of incomplete Na^+ channel inactivation would be the "window" of overlap between steady-state activation and steady-state inactivation. For the IIA Na^+ channel expressed in CHO cells, this window occurs

at −40 to −20 mV (Yang et al., 1992). Later in this paper, we show that "window currents" are important for repetitive firing properties in cells expressing both Na^+ and K^+ currents. However, in the cells described here, which expressed only Na^+ currents, the average recorded plateau began at +21 mV and ended at −19 mV; simulations showed window current does not account for these plateaus.

We therefore sought and found an additional slowly inactivating component of Na^+ current. Because our experiments were conducted in normal extracellular Na^+, it was possible to resolve small components not studied systematically in the experiments of Yang et al. (1992), which were conducted with only 10 mM external Na^+. In Fig. 1 *B*, for instance, roughly 1% of the peak Na^+ currents remain at the end of the 20-ms depolarizing pulses. Because apparent incomplete Na^+ inactivation could conceivably arise from incorrectly subtracted leakage currents, we used several different protocols to confirm and measure the slowly inactivating component (described more fully by Hsu, 1993). This component of Na^+ current was observed whether leak currents were subtracted by using appropriately scaled hyperpolarizing pulses (each of seven cells) or by tetrodotoxin application (one cell). To confirm that the residual currents do not reflect other voltage-dependent conductances, we inverted the Na^+ concentration gradient by using 120 mM internal and 40 mM external Na^+. In each of five experiments, the slow relaxations were now *outward* at potentials between 0 and +40 mV. The slowly inactivating currents were not large; at 100 ms, they averaged 1 to 3% of the peak value.

We found it most reliable to analyze the time course of slow inactivation by measuring Na^+ channel *availability*, that is the fraction of channels that can open because they are not inactivated, during prolonged depolarizations (Hsu, 1993). After inactivation for a variable period at a given inactivation potential, fast inactivation was removed with brief hyperpolarizing prepulses to −100 mV; and Na^+ currents were then measured during a 2.4-ms test pulse to −10 mV. When such data were fit to a single exponential, the time constants for decay were in the range 0.5 to 3 s roughly appropriate to account for the duration of the plateau. We also found an intermediate component of inactivation with time constants on the order of several hundred ms; this component was not studied systematically.

Our experiments included numerical simulations of the voltage trajectories, as described in Materials and Methods. We followed the usual practice of simulating the voltage trajectory for several exemplar cells (for instance, Fig. 2, *A* and *B*) that yielded complete data; the parameters were then verified with data from the entire set of recorded cells. For the present work, the Hodgkin-Huxley equations were modified to include two inactivation parameters, h_1 (fast) and h_2 (slow), in the term $\bar{g}m^3[\epsilon + h_1(1 + \epsilon)]h_2$. Because h_1 decays essentially to zero over a few milliseconds at voltages more positive than −30 mV, the term in brackets above rapidly approaches the parameter ϵ (less than 5% in our experiments) which corresponds to the small fraction of current that inactivates with the slow time constant, $\tau_{h_2,\,Na}$. A possible molecular interpretation of ϵ might be the fraction of time that channels spend in a noninactivating state. For Na^+ activation,

$$m_{\infty,\,Na} = \frac{1}{1 + \exp((V + 28.7)/-7)},$$

$$\alpha_m = \frac{100}{10 + \exp(-(V - 7)/8)},$$

$$\beta_m = 0.01 \exp\left(-\frac{V + 50}{10}\right).$$

For Na^+ inactivation,

$$\epsilon_{Na} = 0.01,$$

$$h_{1\infty,\,Na} = h_{2\infty,\,Na} = \frac{1}{1 + \exp((V + 40)/6)},$$

$$\alpha_{1,\,Na} = 0.0044 \exp\left(-\frac{V + 30}{9.5}\right),$$

$$\beta_{1,\,Na} = \left[1.2 + \frac{96}{1 + 0.087 \exp((V + 61)/5.7)}\right]^{-1},$$

$$\tau_{2,\,Na} = 800 + \tau_{2,\,Na,\,0} \exp\left(-\frac{V}{60}\right), \qquad \tau_{2,\,Na,\,0} = 2000.$$

Parameters for ϵ_{Na} and $\tau_{h_2,\,Na}$ were determined from voltage-clamp experiments described more fully by Hsu (1993). Descriptions of $m_{\infty,\,Na}$, $\tau_{m_1,\,Na}$, and $h_{1\infty,\,Na} = h_{2\infty,\,Na}$ were taken from the work of Yang et al. (1992) and were verified with kinetic analysis of at least five cells under our experimental conditions.

The parameters given above yielded an adequate simulation of the measured plateaus. We summarized the characteristics of 12 plateaus (mean ± SD) in five cells expressing only Na^+ currents, as follows. V_{start} and V_{end} were the potentials at which the slope changed by 5-fold. V_{start} equaled +21.7 ± 7.8 mV (range +37 to +12 mV); the simulated parameter is +21 mV. V_{end} equaled −19.2 ± 9.2 mV (range, −34 to +3 mV); the simulated value is −21 mV. V_{ave} and duration were then defined over the interval between V_{start} and V_{end}. V_{ave} equaled +3.7 ± 9.5 mV (range, −10 to +21 mV); the simulated value is −2 mV. The duration of the plateau equaled 1.92 ± 0.91 s (range, 0.54 to 3.1 s); the simulated value is 1.9 s.

Cells expressing K^+ channels

In cells that were infected with the vaccinia virus vTF7–3 and transfected with the K^+ channel plasmid only (Fig. 1 *B*), there were transient outward currents that strongly resembled those for Shaker H4 channels expressed in oocytes (Iverson et al., 1988; Timpe et al., 1988) and in mammalian cells infected with a recombinant vaccinia virus encoding H4 directly (Leonard et al., 1989; Karschin et al., 1991a). In

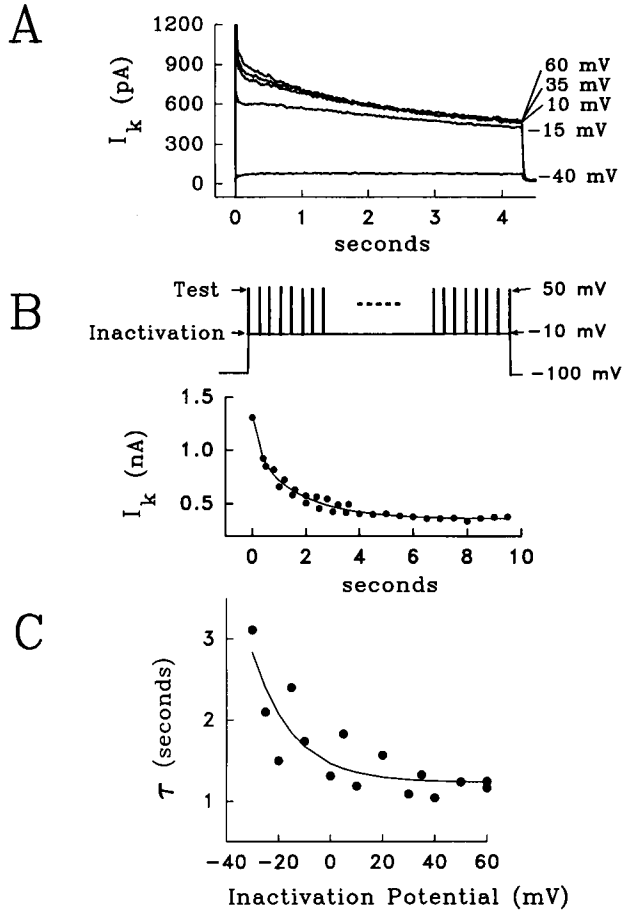

FIGURE 3 Voltage-clamp protocols and data for measuring slow K^+ channel inactivation. (*A*) Jumps to various test potentials at intervals of 25 mV from a holding potential of −100 mV; episodes at intervals of 10 s. The large early peaks of outward current (several nanoamps) are off-scale and have been cut off. (*B*) Data from a different cell, showing protocol and data from a trial with multiple episodes. There was a variable period at the inactivating potential (−10 mV in this example) followed by a test pulse to +50 mV to assess K^+ channel availability. Holding potential, −100 mV. The inactivation time constant is 1.78 s. (*C*) Voltage dependence of the time constants for the cell of *B*; smooth line shows an *e*-fold change for 15.5 mV.

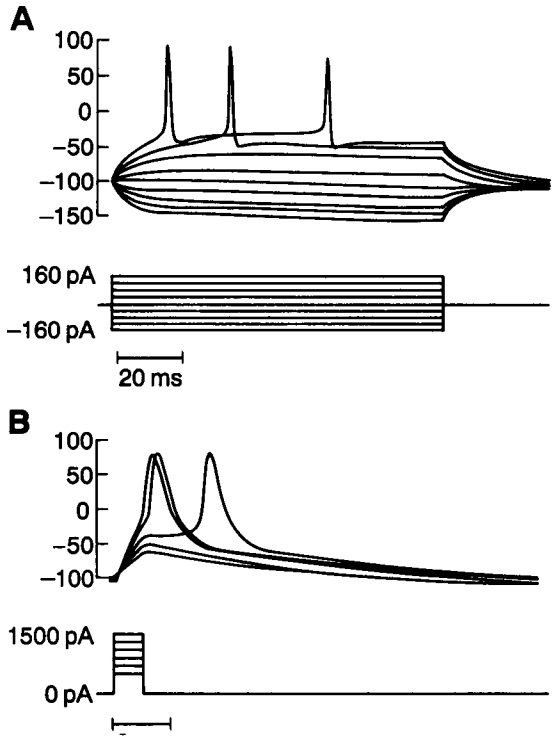

FIGURE 4 Neuron-like action potentials in current-clamp recordings from cells expressing both Na^+ and K^+ channels. (*A*) Records during a series of 105-ms pulses (±40, ±80, ±120, and ±160 pA from a holding current of −230 pA). The hyperpolarizing pulses produced only passive responses; the depolarizing pulses produced action potentials. (*B*) 1.5-ms pulses ranging in amplitude from 500 to 1500 pA from a holding value of −320 pA.

current-clamp mode with zero injected current, however, we noticed an additional phenomenon: the resting potentials were substantially more negative than for cells not expressing K^+ channels. In cells with peak K^+ currents greater than 1 nA at +50 mV, the average resting potential was −26.8 ± 12 mV (mean ± SD, n = 20), in contrast to values of −6.1 ± 6.4 mV (n = 34) for mock-transfected cells, −5.5 ± 5.3 mV (n = 11) for cells transfected with Na^+ channels only, and similar values measured for noninfected cells. These more negative resting potentials can be explained by the presence of a steady K^+ conductance in the window of overlap between activation and inactivation. In a cell with an input resistance of 3 GΩ (a typical value in our mock-transfected cells), the steady conductance would correspond to an additional 0.1 nS, or a small fraction of the average 70-nS peak K^+ conductance at +50 mV, and could not decisively be distinguished from fluctuations in seal resistance. Thus incomplete inactivation of voltage-gated K^+ channels directly contributes to the maintenance of the resting potential.

Additional slow and incomplete inactivation of the Shaker H4 K^+ channel has also been observed by Iverson and Rudy (1990) and termed "C"-type inactivation in a detailed study (Hoshi et al., 1991). To provide the experimental data for quantitative simulations of the voltage trajectories described below, we studied the inactivation of the K^+ currents over a wide time range. Fig. 3 *A* shows a protocol used for these studies. When the voltage is jumped from a hyperpolarized holding potential of −100 mV, there is a rapid decay from the peak outward current >10 nA; the behavior of the subsequent slowly inactivating component is shown. These slowly inactivating K^+ components were larger than the slowly inactivating Na^+ currents described above, ranging between 10 and 20% of the peak K^+ current. However, the crucial range for this study is −50 mV to −20 mV, which accounts for most of the voltage trajectory in a repetitively firing cell (see Fig. 5 *B* below). A protocol that measured K^+ channel availability during prolonged depolarizations was suitable for most of this voltage range (Fig. 3, *B* and *C*).

Cells expressing both Na^+ and K^+ channels

In current-clamp experiments on cells that expressed both channel types (Fig. 4 *A*), both hyperpolarizing current pulses

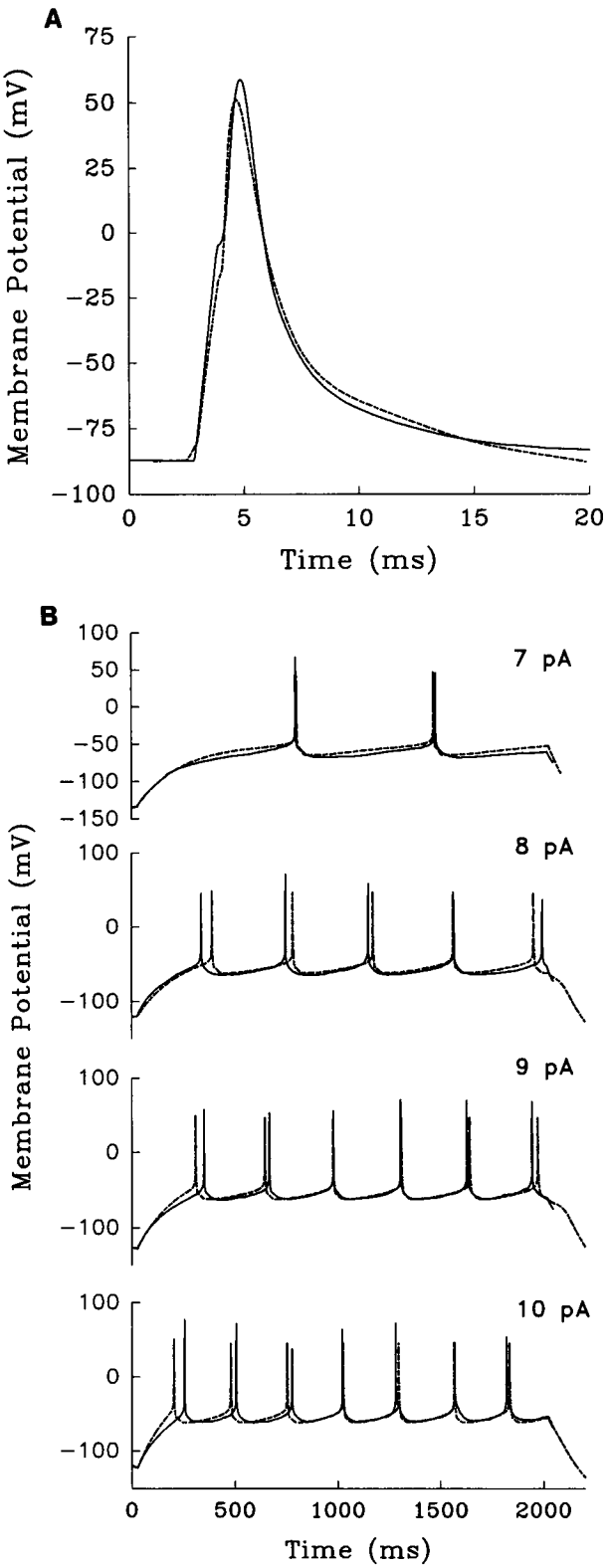

FIGURE 5 Recorded (*solid traces*) and simulated (*dashed traces*) voltage trajectories from a single exemplar cell. (*A*) A single action potential. The cell was stimulated with a 1-nA current for 1 ms, superimposed on a steady current of −0.2 nA. (*B*) Trains of action potentials. The holding current was −30 pA, and the depolarizing currents were applied for 1.9 s at the indicated amplitudes. The peaks of the recorded spikes appear variable, because they were not recorded faithfully at the 1-kHz digitizing rate. For the simulations, parameters are given in the text; also $\bar{g}_{Na} = 70$ pS/(μm)^2, $\bar{g}_K = 40$ pS/(μm)^2, $\bar{g}_{leak} = 0.1$ pS/(μm)^2.

and small depolarizing pulses from holding potentials between −70 and −120 mV produced mostly passive voltage deflections with a time constant determined by the membrane resistance (3.3 ± 0.48 GΩ, mean ± SE for 43 cells; range, 0.3 to 13.6 GΩ,) and capacitance (12.3 ± 1.33 pF; range, 10 to 20 pF). For depolarizations to a threshold value that ranged from −15 to −50 mV (average value was −24.5 mV for 80 cells), the response was an all-or-none action potential with a classical waveform including a peak at +65 to +75 mV and, during maintained depolarizing currents, a brief hyperpolarizing undershoot. (Figs. 4, 5 *B*, and 6). The traces of Fig. 4 *B*, in which action potentials are elicited by a brief current pulse, demonstrate true regenerative behavior: the action potential does not require continued applied current once threshold is reached.

Previous results suggest that repetitive firing would be present in cells possessing transient voltage-dependent conductances for Na^+ and for K^+, if the Na^+ conductance is sufficiently large (Connor and Stevens, 1971a, 1971b, 1971c; H. Hsu, unpublished calculations). Of the 80 cells that produced action potentials in our study, ~20% displayed peak

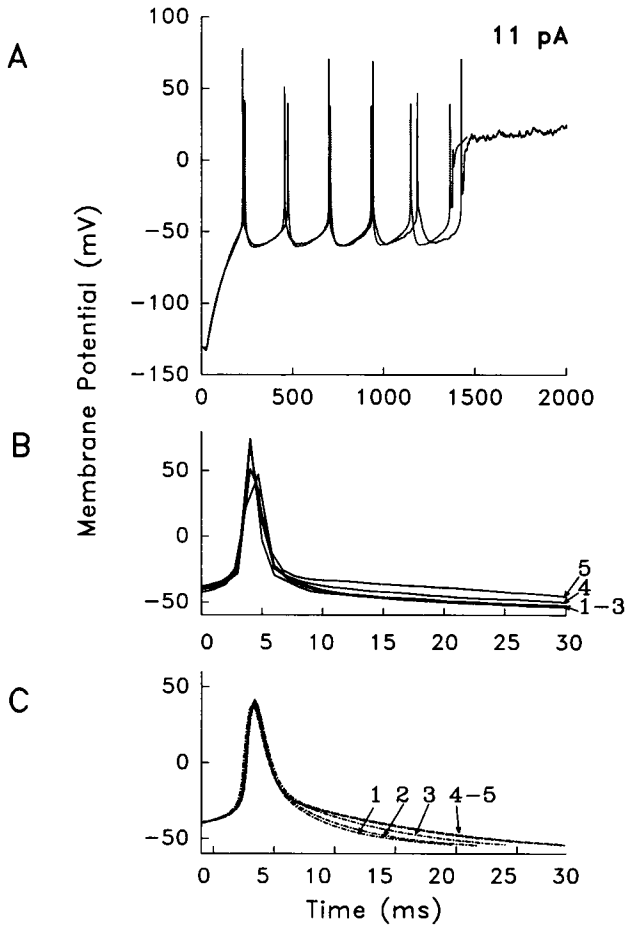

FIGURE 6 An example of lockup. (*A*) Recorded (*solid traces*) and simulated (*dashed traces*) voltage trajectories from the exemplar cell during the same series as Fig. 5. (*B*) Superposition of all the action potential waveforms from *A*. Note the progressive slowing of the hyperpolarizing undershoot. (*C*) Superposition of the simulated action potentials, again showing the progressive slowing of the undershoot.

Na^+ to K^+ current ratios of 2 or greater; and eight of these cells yielded complete current- and voltage-clamp experiments. Each of these cells showed repetitive firing at stable frequencies for at least eight impulses or 2 s (whichever came first) in response to maintained depolarizing currents (Fig. 5). For these cells, the average ratio of peak Na^+ to K^+ currents was 2.01, and the spike threshold averaged −40 mV, versus 0.64 and −21 mV for cells that did not fire repetitively. Firing frequencies f were in the range 0.5–15 Hz in most cells (Fig. 5 *B* is an example) and increased in a roughly linear fashion with stimulus current amplitude I (this is illustrated in Fig. 5 *B*; Fig. 7 *A* shows a plot of f versus I for the exemplar cell). The average slope of this relationship f/I was 0.43 ± 0.14 Hz/pA (mean ± SE). For the cells that fired repetitively, the slope f/I did not depend strongly on the amplitudes of the Na^+ or K^+ conductances or on their ratios; we did however find that this parameter decreased with increasing cell capacitance.

We call attention to two interesting features of the impulse trains. 1) There was a wide frequency range. Firing rates covered at least a 10-fold range in each cell. 2) For large depolarizing currents, the hyperpolarizing undershoot became slower during successive interspike intervals, as shown most clearly in Fig. 6 *A*. Eventually the potential "locked up" at a value near 0 mV and no further impulses were obtained (Fig 6 *A*). Lockup occurred at lower frequencies for cells with lower K^+ conductance.

These voltage trajectories were studied quantitatively with numerical simulation, as described below. However, we first present a qualitative overview of the features that seem to account for the lockup. A voltage-activated K^+ conductance, such as the Shaker H4 expressed in these cells, terminates the action potential by repolarizing the cell. The gradually slower repolarization during successive interspike intervals and eventual lockup after several seconds (Fig. 5, *A* and *B*) would then result from the declining availability of these K^+ channels, due to slow inactivation.

Simulation of repetitive firing

We simulated the voltage trajectories for five cells that yielded our most complete data. Figs. 5 through 7 present recorded and simulated data from a single exemplar cell; only minor changes in the parameters accounted for the other four cells studied in detail. The formal model for the K^+ conductance was identical to that for the Na^+ currents, with two inactivation parameters h_1 (fast) and h_2 (slow): $g_K = \bar{g}_K m^3[\epsilon + h_1(1 - \epsilon)]h_2$. This formalism was chosen because (*a*) fast inactivation does not completely shut the channels but (*b*) that fraction of channels which have undergone slow inactivation do not reopen during subsequent depolarizations. The values for the parameters were based on experiments during this series and on previous data (Leonard et al., 1989). To the equations for Na^+ activation and inactivation, given above, we added these equations for K^+ activation,

$$m_{\infty,K} = \frac{1}{1 + \exp(-(V + 27)/10)},$$

$$\alpha_{m,K} = \left[\frac{320}{1 + \exp[(V + 49)/2]} + 3.6\exp\left(-\frac{V}{25}\right)\right]^{-1},$$

$$\beta_{m,K} = 3.6\left[1 + \exp\left(-\frac{V + 66}{10}\right)\right],$$

and for K^+ inactivation,

$$\epsilon_K = 0.11,$$

$$h_{1\infty,K} = h_{2\infty,K} = \frac{1}{1 + \exp[(V + 29)/3.5]},$$

$$\alpha_{1,K} = 0.018\exp\left(-\frac{V + 70}{17}\right),$$

$$\beta_{1,K} = \left[\frac{385}{1 + \exp[(V + 34)/4]} + 4\right]^{-1},$$

$$\alpha_{2,K} = 3.75 \times 10^{-5}\exp\left(-\frac{V + 40}{15}\right),$$

$$\beta_{2,K} = 0.0025\exp\left(\frac{V}{19}\right).$$

Subscripts of 1 and 2 refer to the parameters governing h_1 and h_2, respectively.

In the simulated voltage trajectories of the exemplar cell (Figs. 5–7) and four other cells, we were able to reproduce the wide range of firing rates and the relation between firing rate and applied current. The slope f/I (Fig. 7 *A*) depends only weakly on Na^+ or K^+ current but shows a roughly inverse dependence on cell size; this agrees with the experimental finding that the slope decreased with larger capacitance (data not shown). The simulations also reproduced the experimentally measured relationship between latency to the first spike and spike train frequency (Fig. 7 *B*). In the simulations, cells with K^+ channel density lower than ~1 nA/pF (+50 mV) locked up at lower firing frequencies than did cells with densities greater than 1 nA/pF, as found experimentally. The simulations reproduced the experimental finding that lockup occurs more quickly as the firing frequency increases (Fig. 7 *C*).

The following points also emerged from the simulations. 1) Between spikes, K^+ conductance remains activated. At 7 Hz, K^+ current is as large as +15 pA (outward), while the algebraic sum of all currents is less than 1 pA and inward. Deactivation (decrease in m with hyperpolarization) and inactivation (decrease in h_1 and h_2 with depolarization and time) of K^+ conductance from −40 mV to −60 mV play a dominant role in determining the firing rate. 2) On the other hand, at frequencies below 2 Hz, the membrane potential is repolarized to E_K, and the remaining K^+ current is negligible (less than 0.5 pA). The precise kinetics of K^+ conductance no longer influence the firing rate. The important parameters

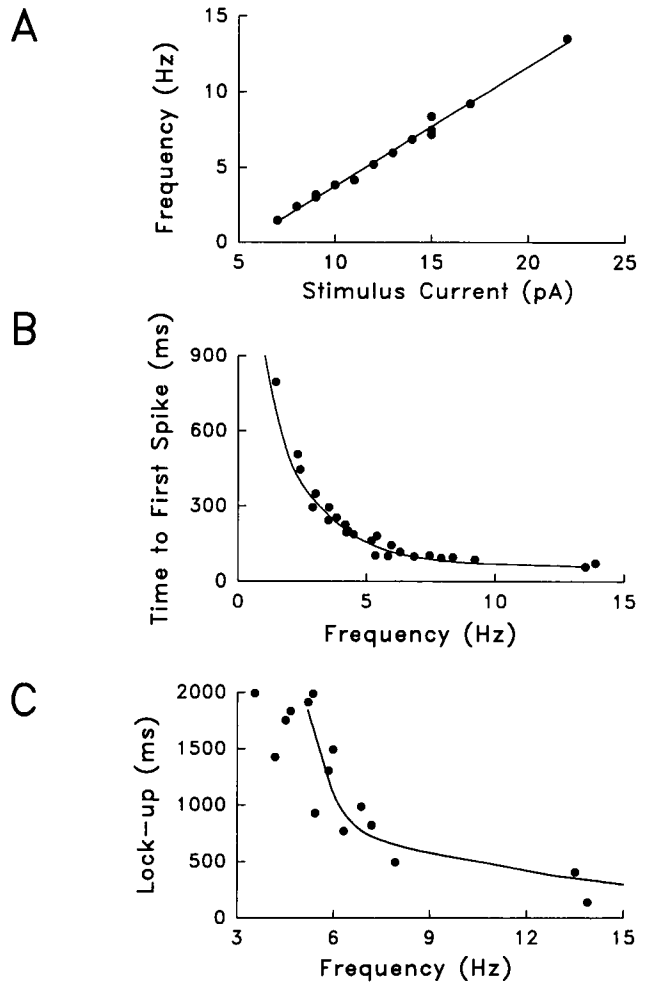

FIGURE 7 Analysis of voltage trajectories in the exemplar cell. (*A*) Firing frequency as a function of stimulus amplitude for recorded data (*symbols*) and simulated data (*lines*). (*B*) Time to first impulse as a function of firing frequency for recorded data (*symbols*) and simulated data (*solid line*). (*C*) Analysis of lockup. Ordinate, time to lockup. Abscissa, firing frequency. Symbols, recorded data; solid line, simulated data.

are the passive resistance and capacitance of the cell. 3) Fig. 8 shows simulated trains of impulses that eventually locked up (*top panels*) and the calculated time course of the inactivation parameters h_1 and h_2 (*bottom panels*). These plots show that slow inactivation of K^+ conductance accounts for the lockup phenomenon at firing rates below 7 Hz (Fig. 8 *A*). With each impulse, h_2 decrements by 3–5%, leading to a cumulative inactivation over several impulses. When insufficient K^+ conductance remains to repolarize the cell, the membrane potential attains a value determined by the injected depolarizing current and by the residual noninactivated Na^+ conductance. Finally, when the interspike interval is long enough to allow recovery even from slow inactivation, the cell in theory will fire indefinitely. Some cells did fire spikes at low frequencies for periods up to 5 min; but these trains were highly variable, presumably because of slow drifts in seal resistance, and were therefore not studied systematically. 4) At firing rates above 7 Hz, fast inactivation of K^+ conductance (controlled by h_1), accounts for the lockup (Fig. 8 *B*). With each action potential, h_1 decrements by 50–55%, then recovers with time constants ranging from 80 ms at −30 mV (as recorded by Leonard et al., 1989) to a peak value of 120 ms at −60 mV. This long recovery time limits the maximum frequency to 15 Hz in most cells. 5) Repetitive firing frequencies did not depend strongly on the detailed kinetics of Na^+ activation and inactivation ($\tau_{m,Na}$, $\tau_{h_1,Na}$, $\tau_{h_2,Na}$) but did require the noninactivating window currents that occur between −20 and −40 mV at the overlap between steady-state activation and inactivation ($m_{\infty,Na}$, $h_{1\infty,Na}$, $h_{2\infty,Na}$).

There remains one untested point in our numerical simulations. The initial hyperpolarizing phases of voltage trajectories during the interspike interval were most accurately simulated by time constants for Na^+ activation/deactivation, $\tau_{m,Na}$, that increased significantly at potentials more negative than −50 mV. This formulation suggests that Na^+ "tail currents" should be relatively long (up to 20 ms) at such potentials. An alternative formulation would assign time constants on this order to an intermediate phase of inactivation. As noted above, we have some evidence for such a phase but have not yet studied it systematically.

There also remain a few discrepancies in our numerical simulations. 1) The voltage trajectories are best simulated with a Na^+ current density for each cell twice that recorded in the voltage-clamp experiments. We believe that this discrepancy arises from artifactually low Na^+ currents measurements, due to lack of series-resistance compensation. 2) The simulated peaks are also 20–30 mV less positive than the recorded peaks; this discrepancy may arise from underdamping in the patch-clamp circuit used in the current-clamp mode (R. Lobdill, Axon Instruments, personal communication).

DISCUSSION

The synthetic neurons display moderately complex encoding properties. When cells express only Na^+ channels, the action potentials have long plateaus that resemble cardiac action potentials (Fig. 2). With only two channel types, a Na^+ and a K^+ channel, the experiments provide the unusual opportunity to study encoding properties of cells lacking the classical "delayed rectifier" found in nearly all excitable cells. Even so, the trajectories include such interesting features as a wide dynamic range of firing frequencies (Fig. 7), time-dependent changes of the action-potential waveform (Fig. 6 *B*) and lockup after several seconds of stimulation (Fig. 6 *A*). The broad dynamic range of firing frequencies resembles that of many real neurons.

Some of these properties might have been predicted on the basis of the original voltage-clamp records from the cloned and expressed Na^+ IIA and Shaker H4 channels; but we lacked the insight to make the right predictions before the measurements and were led instead to several cycles of experiment and simulation. The constraints on our simulations were much more stringent than for real neurons: we could invoke no additional conductances. We conclude that inter-

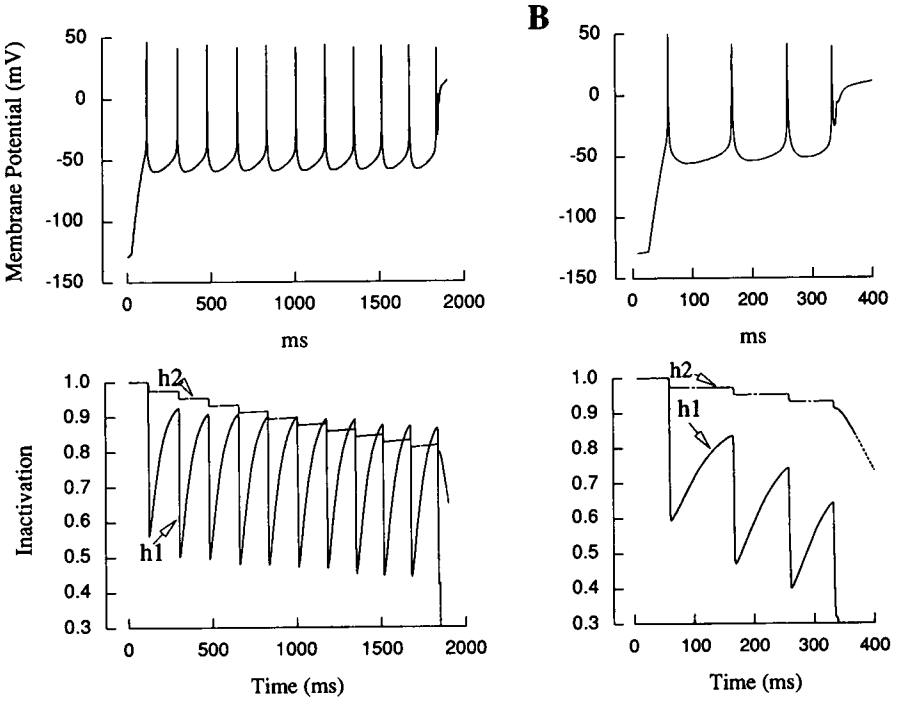

FIGURE 8 Analysis of K^+ inactivation during voltage trajectories leading to lockup. (*A*) At firing rates below 7 Hz, h_1 decrements by 50–55% with each impulse but recovers almost completely during the interspike interval. However, h_2 decrements 3–5% during each spike, leading to a cumulative inactivation over several impulses. When insufficient K^+ conductance remains to repolarize the cell, the membrane potential locks up. (*B*) At firing rates above 7 Hz, changes in h_1 dominate the lockup. With each action potential, h_2 still decrements by 50–55%; but there is insufficient time for complete recovery during the interspike interval.

active experiments and simulations on synthetic neurons provide a decisive strategy for focusing on the important properties of the individual excitable channel populations that account for the voltage trajectories in a cell.

In general, we acknowledge that our equations and parameters, based on the Hodgkin-Huxley (1952) formalism, may represent only one of several possible formal descriptions that would adequately simulate the voltage trajectories. However, we devoted considerable effort to simulations that omitted slowly inactivating Na^+ and K^+ conductances; such models could not account for the plateau and lockup. We therefore have confidence in the conclusion that slow channel kinetics do underlie these slow components of the voltage trajectories. Furthermore, the noninactivating Na^+ window currents were essential for explaining the long interspike intervals we observed; and the noninactivating K^+ window currents explained the negative resting potentials.

Role of transient K^+ currents in repetitive firing

It has long been thought that transient K^+ channels ("A" channels) play an important role in determining repetitive firing activity of neurons by broadening the range of input currents over which repetitive firing occurs (Connor and Stevens, 1971a, 1971b, 1971c). Our study confirms this concept; for instance, our synthetic neurons fire repetitively over a wider frequency range than does the standard Hodgkin-Huxley axon whose only K^+ conductance is a maintained one (Huxley, 1959). Shaker H4 channels activate at a considerably more positive voltage than do most A channels in neurons (Rudy, 1988); nonetheless, once they are activated by an action potential, they appear to deactivate so slowly that they do contribute to the next interspike interval. It would be instructive to repeat the present experiments with a transient K^+ channel that activates at more negative potentials. It is also thought that, for larger depolarizations, the transient K^+ channels inactivate and no longer control the voltage trajectory during the interspike interval (Connor and Stevens, 1971a, 1971b, 1971c). Our neurons lock up when the K^+ conductance inactivates. We predict that expression of an additional maintained K^+ conductance ("delayed rectifier") which would decrease the tendency to lock up and would allow higher firing frequencies. Experiments in progress are aimed at introducing such a conductance.

Relevance of synthetic neurons

The data and simulations suggest that slow inactivation (termed C-type inactivation by Hoshi et al. (1991)) of transient K^+ currents is not an epiphenomenon but could play a role in encoding properties of real neurons. For a typical sustained depolarization, many times more charge flows through these channels during the long, slow phase than during the larger but much briefer early peak. On the other hand, inactivation of transient K^+ currents has previously been invoked to explain spike broadening by depolarization (Belluzzi et al., 1985). Such broadening may have functional consequences, because it increases the amount of transmitter released from presynaptic terminals (Klein et al., 1982; Augustine, 1990; Kaang et al., 1992).

C-type inactivation also occurs for K^+ channels, such as Kv3, that are maintained for several tens of milliseconds (Marom et al., 1992). In the case of Kv3, C-type inactivation can be modulated (Marom et al., 1992), raising the possibility that external influences could control the effects of such inactivation on voltage trajectories.

The role of high impedance

The CHO cells used in the present studies have few or no endogenous channels. If only Na^+ channels are expressed, membrane potentials are sensitive to even the small component of slowly inactivating Na^+ current. Our simulations show how the plateau results. While this low background conductance contributes to the interesting encoding mechanisms we have observed, is it relevant to real excitable cells? The literature suggests that it is. As a first example, Hille (1991, pp. 128–129 and 193–197) argues that the low density of background conductance 1) allows cardiac muscle to spend a high percentage of time depolarized with only a moderate metabolic load and 2) allows modulation of small currents to influence encoding properties. Some experiments in the literature suggest that the plateau phase of the cardiac action potential is governed by incomplete Na^+ channel inactivation as well as by the slow Ca^{2+} conductance (Grant and Starmer, 1987; Liu et al., 1992). The experiment of Fig. 2 is relevant to this point, because we know that Na^+ channels are the only ones open during the plateau. As a second example of the relevance of low background conductance, recent patch-clamp recordings in brain slices reveal much lower background conductances than previously suspected (Blanton et al., 1989; Edwards et al., 1989; Andersen et al., 1990). Thus our experiments may provide a model for neurons as well as cardiac cells. Incomplete Na^+ channel inactivation has often been observed with both native and expressed Na^+ channels (Chandler and Meves, 1970a, 1970b, 1970c, 1970d; Rudy, 1978; Matteson and Armstrong, 1982; Patlak and Ortiz, 1985, 1986; Llinás, 1988; Moorman et al., 1990; Zhou et al., 1991). As a third example of the relevance of low background conductance, we note that the small fraction of voltage-gated K^+ channels open at −27 mV was enough to set the membrane potential to this value in our synthetic neurons and that similar phenomena have been described for T-lymphocytes (Leonard et al., 1992).

Between impulses, a neuron's membrane potential is typically between −40 and −60 mV. Our simulations demonstrate that kinetics of channel conductance at these potentials directly determine the firing rate. A small change in these kinetics can dramatically alter dynamic properties. Many voltage-dependent channels have window currents that do not inactivate. In cells with low impedance, these sustained currents are negligible compared to the background current. In the synthetic neurons, the high impedance unmasks these small, slowly changing currents. They contribute significantly to the shape of the interspike waveform and the firing rate. The high impedance enables the cell to integrate currents just a few picoamps in amplitude.

Limitations and possibilities of the synthetic neuron system

Real neurons have many more channel types than the synthetic neurons reported here (Llinás, 1988). The vaccinia system has also been used to introduce serotonin $5HT_{1A}$ receptors into mammalian cardiac cells, where they couple via endogenous G proteins to a class of endogenous K^+ channels important in regulating impulse frequency (Karschin et al., 1991b). Thus it also seems possible to employ vaccinia or other mammalian cell expression systems to investigate the control of encoding properties by neurotransmitters in cells that are already endowed with a set of endogenous channels, receptors, or transporters.

The major limitation of the vaccinia expression system is the wide variability of expression levels among cells in the population. Only 20% of the cells in our experiments expressed Na^+ and K^+ channels in the range of ratios that gave repetitive firing. The percentage of satisfactory expression would presumably decrease even further if three or more channel types were employed. We suspect that the most appropriate system will be one in which 1) a cell line is constructed that stably expresses a basic set of channels—for instance, the two studied here—and 2) additional channels are added using a flexible and rapid transient expression system such as vaccinia virus.

We thank O. Elroy-Stein and B. Moss for furnishing vTF7–3, pTM1, and pTM1lac and for much helpful discussion, C. Miller for the H4 plasmid and O. Bernander, F. A. Dodge, Jr., G. Laurent, and C. Koch for discussion.

Supported by grants from the National Institute of Mental Health (MH-49176), the Office of Naval Research, and the Multiple Sclerosis Society and by fellowships from the Pew Foundation (to H. Hsu), the Muscular Dystrophy Association (to X.-c. Yang), the Alexander von Humboldt Foundation (to A. Karschin), the Department of Energy (to E. Huang), and the American Heart Association (to B. Ho).

REFERENCES

Andersen, P., M. Raastad, and J. F. Storm. 1990. Excitatory synaptic integration in hippocampal pyramids and dentate granule cells. *Cold Spring Harbor Symp. Quant. Biol.* 55:81–96.

Augustine, G. J. 1990. Regulation of transmitter release at the giant squid synapse by presynaptic delayed rectifier potassium current. *J. Physiol. (Lond.).* 31:33–364.

Auld, V., A. L. Goldin, D. S. Krafte, J. Marshall, J. M. Dunn, W. A. Catterall, N. Davidson, H. A. Lester, and R. J. Dunn. 1988. A rat brain Na channel α subunit with novel gating properties. *Neuron.* 1:449–461.

Auld, V. J., A. L. Goldin, D. S. Krafte, J. Marshall, J. M. Dunn, W. A. Catterall, H. A. Lester, N. Davidson, and R. J. Dunn. 1990. A neutral amino acid change in segment IIS4 dramatically alters the gating properties of the voltage-dependent sodium channel. *Proc. Natl. Acad. Sci. USA.* 87:323–327.

Belluzzi, O., O. Sacchi, and E. Wanke. 1985. Identification of delayed potassium and calcium currents in the rat sympathetic neurone under voltage clamp. *J. Physiol. (Lond.).* 358:109–129.

Blanton, M. G., J. J. Loturco, and A. R. Kriegstein. 1989. Whole cell recording from neurons in slices of reptilian and mammalian cerebral cortex. *J. Neurosci.* 30:203–210.

Chandler, W. K., and H. Meves. 1970a. Sodium and potassium currents in squid axons perfused with flouride solution. *J. Physiol. (Lond.).* 211: 623–652.

Chandler, W. K., and H. Meves. 1970b. Evidence for two types of sodium conductance in axons perfused with sodium flouride solution. *J. Physiol. (Lond.).* 211:653–678.

Chandler, W. K., and H. Meves. 1970c. Rate constants associated with changes in sodium conductance in axons perfused with sodium flouride solution. *J. Physiol. (Lond.).* 211:679–705.

Chandler, W. K., and H. Meves. 1970d. Slow changes in membrane permeability and long-lasting action potentials in axons perfused with flouride solutions. *J. Physiol. (Lond.).* 211:707–728.

Connor, J. A., and C. F. Stevens. 1971a. Inward and delayed outward membrane currents in isolated neural somata under voltage clamp. *J. Physiol. (Lond.).* 213:1–19.

Connor, J. A., and C. F. Stevens. 1971b. Voltage clamp studies of a transient outward membrane current in gastropod neural somata. *J. Physiol. (Lond.).* 213:21–30.

Connor, J. A., and C. F. Stevens. 1971c.. Prediction of repetitive firing behavior from voltage clamp data on an isolated neurone soma. *J. Physiol. (Lond.).* 213:31–53.

Edwards, F. A., A. Konnerth, B. Sakmann, and T. Takahashi. 1989.. A thin slice preparation for patch clamp recordings from neurons of the mammalian central nervous system. *Pfluegers Arch. Eur. J. Physiol.* 414:600–612.

Elroy-Stein, O., T. R. Fuerst, and B. Moss. 1989. Cap-independent translation of mRNA conferred by encephalomyocarditis virus 5′ sequence improves the performance of the vaccinia virus/bacteriophage T7 hybrid expression system. *Proc. Natl. Acad. Sci. USA.* 86:6126–6130.

Grant, A. O., and C. F. Starmer. 1987. Mechanisms of closure of cardiac sodium channels in rabbit ventricular myocytes: single channel analysis. *Circ. Res.* 60:897–913.

Hille, B. 1991. Ionic Channels in Excitable Membranes. 2nd edition. Sinauer Associates, Sunderland, MA.

Hines, M. 1989. A program for simulation of nerve equations with branching geometries. *Int. J. Biomed. Comput.* 24:55–68.

Hodgkin, A. L., and A. F. Huxley. 1952. A quantitative description of membrane current and its application to conduction and excitation in nerve. *J. Physiol. (Lond.)* 117:500–544.

Hoshi, T., W. N. Zagotta, and R. W. Aldrich. 1991. 2 types of inactivation in Shaker K^+ channels–effects of alterations. *Neuron.* 7:547–556.

Hsu, H. 1993. Properties of the first genetically engineered neuron. Ph.D. dissertation. California Institute of Technology, Pasadena, CA.

Huxley, A. F. 1959. Ion movements during nerve activity. *Ann. NY Acad. Sci.* 81:221–246.

Iverson, L. E., and B. Rudy. 1990. The role of the divergent amino and carboxyl domains on the inactivation properties of potassium channels derived from the Shaker gene of *Drosophila. J. Neurosci.* 10:2903–2916.

Iverson, L., M. A. Tanouye, H. A. Lester, N. Davidson, and B. Rudy. 1988. A-type potassium channels expressed from Shaker locus cDNA. *Proc. Natl. Acad. Sci. USA.* 85:5723–5727.

Kamb, A., L. E. Iverson, and M. A. Tanouye. 1987. Molecular characterization of Shaker, a *Drosophila* gene that encodes a potassium channel. *Cell.* 50:405–413.

Kaang, B. K., P. J. Pfaffinger, S. G. N. Grant, E. R. Kandel, and Y. Furukawa. 1992. Overexpression of an *Aplysia* Shaker K^+ channel gene modifies the electrical properties and synaptic efficacy of identified *Aplysia* neurons. *Proc. Natl. Acad. Sci. USA.* 89:1133–1137.

Karschin, A., J. Aiyar, A. Gouin, N. Davidson, and H. A. Lester. 1991a. K^+ channel expression in primary cell cultures mediated by vaccinia virus. *FEBS Lett.* 278:229–233.

Karschin, A., B. Ho, C. Labarca, O. Elroy-Stein, B. Moss, N. Davidson, and H. A. Lester. 1991b. Heterologously expressed serotonin 1A receptors couple to muscarinic K^+ channels in heart. *Proc. Natl. Acad. Sci. USA.* 88:5694–5698.

Klaiber, K., N. Williams, T. M. Roberts, D. M. Papazian, L. Y. Jan, and C. Miller. 1990. Functional expression of *Shaker* K^+ channels in a baculovirus-infected insect cell line. *Neuron.* 5:221–226.

Klein, M., J. Camardo, and E. R. Kandel. 1982. Serotonin modulates a specific potassium current in the sensory neurons that show presynaptic facilitation in *Aplysia. Proc. Natl. Acad. Sci. USA.* 79:5713–5717.

Krafte, D. A., T. P. Snutch, J. P. Leonard, N. Davidson, and H. A. Lester. 1988. Evidence for the involvement of more than one mRNA species in controlling the inactivation process of rat and rabbit brain Na channels expressed in *Xenopus* oocytes. *J. Neurosci.* 8:2859–2868.

Krafte, D. S., A. L. Goldin, V. J. Auld, R. J. Dunn, N. Davidson, and H. A. Lester. 1990. Inactivation of cloned Na channels expressed in *Xenopus* oocytes. *J. Gen. Physiol.* 96:689–706.

Leonard, R. J., A. Karschin, J. Aiyar, N. Davidson, M. A. Tanouye, L. Thomas, G. Thomas, and H. A. Lester. 1989. Expression of Shaker potassium channels in mammalian cells using recombinant vaccinia virus. *Proc. Natl. Acad. Sci. USA.* 86:7629–7633.

Leonard, R. J., M. L. Garcia, R. S. Slaughter, and J. P. Reuben. 1992. Selective blockers of voltage-gated K+ channels depolarize human lymphocytes. Mechanism of the antiproliferative effect of charybdotoxin. *Proc. Natl. Acad. Sci. USA.* 89:10094–10098.

Liu, Y. M., DeFelice, L. J., and Mazzanti, M. 1992. Na channels that remain open throughout the cardiac action-potential plateau. *Biophys. J.* 63:654–662.

Llinás, R. 1988. The intrinsic electrophysiological properties of mammalian neurons: insights into central nervous system function. *Science (Wash. DC).* 242:1654–1664.

Marom, S., S. A. N. Goldstein, J. Kapper, and I. Levitan. 1992. Mechanism and modulation of inactivation of the Kv3 potassium channel. *Recept. Channels* 1:81–88.

Matteson, D. R., and C. M. Armstrong. 1982. Evidence for a population of sleepy sodium channels in squid axons at low temperatures. *J. Gen. Physiol.* 79:739–758.

Moss, B., O. Elroy-Stein, T. Mizukami, W. A. Alexander, and T. R. Fuerst. 1990. New mammalian expression vectors. *Nature (Lond.).* 348:91–92

Moorman, J. R., G. E. Kirsch, A. M. J. VanDongen, R. H. Joho, and A. M. Brown. 1990. Fast and slow gating of sodium channels encoded by a single mRNA. *Neuron.* 4:243–252.

Patlak, J., and M. Ortiz. 1985. Slow currents through single sodium channels of the adult rat heart. *J. Gen. Physiol.* 86:89–104.

Patlak, J., and M. Ortiz. 1986. Two modes of gating during late Na^+ channel currents in frog sartorius muscle. *J. Gen. Physiol.* 87:305–326.

Rudy, B. 1978. Slow inactivation of the sodium conductance in squid giant axons. Pronase resistance. *J. Physiol. (Lond.).* 283:1–21.

Rudy, B. 1988. Diversity and ubiquity of K channels. *Neuroscience.* 25: 729–749.

Timpe, L. C., T. L. Schwarz, B. L. Tempel, D. M. Papazian, Y. N. Jan, and L. Y. Jan. 1988. Expression of functional potassium channels from *Shaker* cDNA in *Xenopus* oocytes. *Nature (Lond.).* 331:143–145.

Yang, X.-C., C. Labarca, J. Nargeot, B. Ho, N. Davidson, and H. A. Lester. 1992. Cell-specific posttranslational events affect functional expression at the plasma membrane but not tetrodotoxin sensitivity of the rat brain IIA sodium channel α subunit expressed in mammalian cells. *J. Neurosci.* 12:268–277.

Zhou, J., J. F. Potts, J. S. Trimmer, W. S. Agnew, and F. J. Sigworth. 1991. Multiple gating modes and the effect of modulating factors on the μI sodium channel. *Neuron.* 7:775–785.